Atmos. Chem. Phys. Discuss., 9, 11413–11440, 2009
www.atmos-chem-phys-discuss.net/9/11413/2009/

Atmospheric Chemistry and Physics Discussions

This discussion paper is/has been under review for the journal *Atmospheric Chemistry and Physics (ACP)*. Please refer to the corresponding final paper in *ACP* if available.

An intensive study of aerosol optical properties in Beijing urban area

X. He[1], C. Li[1], A. K. H. Lau[2], Z. Deng[1], J. Mao[1], M. Wang[1], and X. Liu[1]

[1]Dept. of Atmospheric Sciences, School of Physics, Peking University (PKU), Beijing, China
[2]ENVF/IENV, The Hong Kong University of Science and Technology (HKUST), Hong Kong

Received: 5 February 2009 – Accepted: 24 April 2009 – Published: 8 May 2009

Correspondence to: C. Li (ccli@pku.edu.cn)

Published by Copernicus Publications on behalf of the European Geosciences Union.

Abstract

In order to quantify the aerosol impact on climate, a range of aerosol parameters is required. In this paper, two-year ground-based observations of aerosol optical properties are conducted at an urban site in Beijing of China. Aerosol absorption coefficient (σ_a) and scattering coefficient (σ_s), as well as single scattering albedo (ω) are analyzed for characterizing Beijing urban aerosol. Two-year averages (and standard deviations) for σ_a, σ_s and ω are 56±49 Mm^{-1}, 288±281 Mm^{-1} and 0.80±0.09, respectively. Meanwhile, there is a distinct diurnal variation for σ_a, with its minimum occurs about 14:00 to 15:00 and maximum in the evening. While, σ_s peaks in late morning and the minimum occurs in the evening. σ_s in summer is higher than that in winter. ω in summer is higher than that in winter except before 07:00 a.m. and it peaks in the early afternoon. Both σ_a and σ_s show strong dependence on local wind in four seasons. When the wind blows from north with low speed (0–4 m/s), both σ_a and σ_s are high, while very low with wind speed higher than 4 m/s. When the wind blows from south with low speed (0–4 m/s), σ_a and σ_s are intermediate. ω also shows wind dependence to some extent though not as strong as σ_a and σ_s.

1 Introduction

Aerosols have been gaining substantial attention recently due to their complicated roles in global climate. It is generally accepted that aerosols affect the earth's energy budget mainly through directly scattering the incoming solar radiation back into space and indirectly enhancing cloud reflectivity by increasing the number concentration of cloud droplets (Penner et al., 2001; IPCC, 2001; Kaufman et al., 2002). However, their combined effect is very complicated and large uncertainties remain in the simulation of climate system. For example, the existence of absorptive aerosols such as black carbon (BC) may lead to local heating in the atmosphere as well as absorption and re-emission of long-wave infrared radiation that enhances the greenhouse effect and can

ACPD

9, 11413–11440, 2009

then partially counteract the cooling effect of sulfates aerosols. Jacobson (2001) concluded that the warming effect of BC may nearly balance the net cooling effect of other anthropogenic aerosol constituents. BC is released usually from combustion of fossil fuels, primarily from diesel, coal, and biomass burning. It is inert in the atmosphere as a result of its chemical structure. Generally, BC is a component of fine particle thus can be a great threat to human health because it can be inhaled deep into the lungs. It has been reported that the BC aerosols can also alter precipitation, surface air temperature and large-scale circulation and hydrologic cycle with significant regional climate effects (Menon et al., 2002). Single scattering albedo (ω), which is defined as the ratio of scattering coefficient (σ_s) to the total extinction coefficient, is another optical parameter to characterize the aerosol optical properties. For BC, ω is about 0.2, while nearly 1.0 for sulfate aerosol. Aerosols have a negative Top of Atmosphere (TOA) forcing when ω exceeds 0.95, and a positive TOA forcing if ω<0.85, and for the intermediate values, the net effect can change from negative to positive forcing depending on the cloud fraction, surface albedo, and the cloud distribution (Ramanathan et al., 2001a). The ω of the aerosols in the Northern Hemisphere are in the range of 0.85 to 0.95 (Ramanathan et al., 2001b). Single scattering albedo is one key parameter in atmospheric aerosol optical depth retrieval from satellite remote sensing. A value ~0.95 of the ω was used in the operational aerosol retrieval algorithm from Moderate Resolution Imaging Spectroradiometer (MODIS) for the urban aerosol over the whole eastern China (Kaufman et al., 1997; Chu et al., 2003). However, the improved second-generation operational algorithm adopted 0.85 for the urban aerosol over this region (Levy et al., 2007) .

Beijing, one of the largest cities in the world, has been experiencing the problem of severe aerosols loading as a result of rapid economic development, population expansion and urbanization in the last 30 years (Chan et al., 2008), which will pose great effects on climate (Zhou et al., 2004; Crutzen, 2004). The Air Pollution Index (API) released by the Beijing Municipal Environmental Protection Bureau indicates that the main pollutant in Beijing is respirable suspended particle (RSP) (http://www.bjepb.gov.cn/). It was reported that the hourly average PM_{10} could be as

ACPD
9, 11413–11440, 2009

large as 400 $\mu g\,m^{-3}$(Ando et al., 1994; He et al., 2001; Shi et al., 2003). The Beijing aerosol contain a high amount of black carbon (Bergin et al., 2001), dust from construction activities (He et al., 2001), coal burning particles, factory and vehicle exhaust particles (Zhang et al., 1998). The impairment of visibility is one of the most notable effects of aerosol. As the key factors for evaluating atmospheric pollution, aerosol optical depth (AOD) has increased dramatically from 1961 to 1990 (Luo et al., 2001). Li et al. (2003) reported a yearly mean AOD of 0.5. In Beijing, although different values of ω have been observed based on different instruments and measuring conditions, the ω is comparatively low. According to one-week surface observation made in June 1999, a low ω value of 0.81 was obtained by in situ surface observations in Beijing (Bergin et al., 2001). Qiu et al. (2004) reported that ω decreases from ~0.85 to <0.83 over Beijing from 1996–2001. The ω value derived from combined one-wavelength Raman lidar and Sun photometer measurements in Beijing in January 2005 was as low as 0.75 at the wavelength of 525 nm and a downward trend since 2001 (Müller et al., 2006).

The spatial and temporal distribution of aerosols requires analysis of local and regional meteorology condition, especially wind direction, wind speed, topography, and atmospheric stability. The wind plays an important role in diluting and transporting the air pollutants. It determines how quickly the pollutants mix with ambient air and how fast they move away from their sources. Although the relationship between meteorology and air pollution have been investigated, such as ozone (Comrie, 1994; Eder et al., 1994), BC (Wiliam et al., 1997; Ramachandran et al., 2007), aerosol (Elminir, 2005; Hartog et al., 2005), the dependence of urban aerosol optical properties on the meteorology in Beijing is rarely studied.

This work presents the variations of absorption coefficient, scattering coefficient and single scattering albedo and examines the relationship between wind and aerosol optical properties (σ_a, σ_s and ω) from two years' observation in Beijing. Diurnal, seasonal and annual variations are also analyzed. In Sect. 2, site, instruments and data are introduced. In Sect. 3, the diurnal variation and statistics of aerosol absorption coefficient and scattering coefficient as well as single scattering albedo are shown, and the

ACPD
9, 11413–11440, 2009

wind dependency is also analyzed.

2 Data and methodology

2.1 Site descriptions

Figure 1 presents the main part of the map of North China. The municipality of Beijing borders Hebei Province to the north, west, south, and for a small section in the east, and Tianjin Municipality to the southeast. The background image shows the annual average of aerosol optical depth (AOD) in 2006 over the region. The data are from the Level 2 products (Version 5) of MODIS onboard the Terra and Aqua satellites Platform derived by The National Aeronautics and Space Administration of the United Staes (NASA) (http://modis-atmos.gsfc.nasa.gov/). The contours with the value 0.4~0.5 divide the area into two parts: plateau and mountains in the north and plain in the south. The AOD values over the north plateau (the blue part in the figure) are usually less than 0.4, however, those over the North China Plain (the yellow and the red parts in the figure) are almost larger than 0.6. Four main cities in this region are shown in the figure: Beijing (BJ), Tianjin (TJ), Shijiazhuang (SJZ) and Baoding (BD). Every city owns a higher AOD center (larger than 0.8 or 0.9).

The urban area of Beijing is located in the joint area of the North China Plain and the Inner Mongolia plateau, and surrounded by the Taihang Mountains on the west, Yanshan Mountains on the north. Beijing is a megacity, with a population of more than 15 000 000, facing severe aerosol pollution. During the period from January 2005 to December 2006, an intensive observation of aerosol optical properties was conducted at Peking University (PKU, 39°59′30″ N, 116°18′39″ E), which is on the northeast of Beijing. Peking University is surrounded by a number of residential and business complexes, and there are no factories nearby. As shown in Fig. 1, the sampling site (shown in the figure with a star) is on the edge of a heavily polluted region with the yearly averaged AOD values larger than 0.8. The measurement site at PKU does not have

ACPD
9, 11413–11440, 2009

any very tall buildings nearby and therefore the measurements can reflect the average conditions over the northeast part of the urban area of Beijing. The emitted particles in this region are mainly attributed to vehicular traffic, construction site and cooking exhaust from families and restaurants in whole year, and central and domestic heating in winter season.

2.2 Measurements and instrumentations

All of the instruments, including Nephelometer, Aethalometer and automatic weather station, were located on the roof of Physics Building about 30 m from the ground. The nephelometer and aethalometer were installed in a room built on the roof with the inlets over the room.

The integrating Nephelometer (Model M9003, Ecotech, Australia) was used to measure the light scattering coefficient at the single wavelength of 525 nm with scattering angles between 10° and 170°, and no size-selective inlet was used. The measured values were automatically adjusted in real-time for different air density in fixed airflow volume by on-board temperature and pressure sensors. A background (zero) calibration was performed at midnight every day automatically. The span calibration was made at intervals of 10–30 days using particle-free gas. If there was a big deviation arising in zero and span calibration, a full calibration was executed. The particle inlet had a processor-controlled automatic heater and an RH threshold of 60% was set to prevent liquid particles going into the optical cell of the instrument.

An Aethalometer (Model AE16, Magee Scientific, USA) was used to measure the concentration of black carbon and the absorption coefficient. The aethalometer measured the attenuation of a beam of light transmitted through the sample collected on the quart fiber filter while the filter was continuously collecting samples. The measured attenuation is linearly proportional to the mass of black carbon in the filter deposit. The instrument operated in the near-infrared at the wavelength of 880 nm at a flow rate of 3 L per minute, which was affected less by other non-absorbing aerosols. The exclusive drawback arises that the multiple scatterings within the fiber filter do not overcome

completely the scattering interference with measurements, and another problem is that the particles on the filter are not in their natural condition (Mao et al., 2006). Data was recorded as concentrations of black carbon in $\mu g/m^3$. According to the comparison result between an aethalometer at the wavelength of 880 nm and a photoacoustic spectrometer (PAS, an instrument which provides highly sensitive absorption measurements without interference by scattering signals) operating at 532 nm in South China (The Aethalometer Handbook, 2005), there is a good agreement between the absorption coefficient (σ_a, Mm^{-1}) and black carbon concentration([BC], $\mu g/m^3$):

$$\sigma_a = 8.28 \times [BC] + 2.23, R^2 = 0.92, \quad (1)$$

where 8.28 is the conversion factor in m^2/g. Different values of the factor have been adopted at different sites, e.g., 10 m^2/g often used for urban aerosols (Moosmuller et al., 1998), 8–10 m^2/g (at 550 nm) in Mexico City (Barnard et al., 2007), 8.5 m^2/g from BRAVO (Big Bend Regional Aerosol and Visibility Observation Study) (Arnott et al., 2003). The conversion factor 8.28 m^2/g was also used in a study by Yan et al. (2008) for obtaining the aerosol absorption over a rural site in North China. Lacking of the comparison at Beijing at the same time, we took 8.28 m^2/g as the conversion factor at the wavelength of 532 nm. From the above references we know its error may introduce 10–20% error on the estimation of aerosol absorption coefficients.

Meteorological data were obtained every 12 s from an automatic weather station made by Vaisala Ltd., which measured wind speed (WS), wind direction (WD) and other parameters such as relative humidity (RH), precipitation amount and barometric pressure.

All of the scattering and absorption coefficient data were recorded at 5-min intervals. The data have been manually edited to remove invalid data resulting from instrumental problems or affected by dust storm or rain.

Single scattering albedo is defined as the ratio of the scattering coefficient to the total extinction coefficient, which is the sum of scattering coefficient and absorption

ACPD
9, 11413–11440, 2009

coefficient

$$\omega(\lambda) = \sigma_s(\lambda)/(\sigma_s(\lambda) + \sigma_a(\lambda)). \quad (2)$$

The scattering coefficient was observed at 525 nm and the absorption coefficient was obtained at 532 nm. As the absorption coefficient is not sensitive to the small variation of wavelength (532–525 nm), the results of single scattering albedo in this study are at 525 nm.

3 Results and discussion

3.1 Absorption coefficient

In Fig. 2 the averaged diurnal variation of σ_a in summer and winter obtained at Beijing during 2005–2006 is plotted with standard deviation as error bar. As can be seen from the figure, the absorption coefficient exhibits strong diurnal variation both in summer and winter, with higher value in night and lower value in the daytime. At the early morning, 2-year mean absorption coefficient is about 75 Mm^{-1} (inverse mega-meter: 10^{-6} m^{-1}). The lowest σ_a of 37 Mm^{-1} occurs in the afternoon (14:00–15:00), which is only half of the value in the mid-night. Note that, in general, the black carbon mainly comes from incomplete combustion of fuels, especially diesel. Heavy trucks which produce a large amount of BC are only permitted to pass through the urban Beijing from 19:00 to 07:00. Meanwhile, aerosol concentration is also dependent on the stability of boundary layer, which is usually unstable in the daytime while stable at night. Beijing urban boundary layer showed diurnal pattern with low height values at night and much higher values during the daytime (Benjamin et al., 2006).

Annual mean σ_a is 58±52 Mm^{-1} in 2005 (Table 2), which is a little higher than that of 2006 with the value of 53±46 Mm^{-1}. Our result is two-fifth lower than Bergin et al.'s (2001) surface observation in June 1999 in Beijing, and is two time larger than rural Beijing (Yan et al., 2008) (Table 1). As seen in Table 2, the σ_a in winter and autumn is

higher than that in spring and summer. The heating in winter from November to March contributes to the BC concentration by the direct emission of coal consumption.

Figure 3 presents the wind dependence of absorption coefficient for different seasons. In this work, March, April and May is regarded as spring; June, July and August as summer; September, October and November as autumn; December, January and February as winter. In the figure, a polar coordinate system is plotted depending on the wind speed (0–8 m/s) and wind direction (0–360°). The color on the plot represents the magnitude of the variable (absorption coefficient), and the unit of the color bar is Mm^{-1}. The direction angle 0° of the plot means the wind blows from the north, 90° means the wind is from the east. The hourly data are used in the plot. Figure 3a, b, c and d are for spring, summer, autumn and winter respectively. The black line represents the relative occurrence frequency of wind direction. We define the absorption coefficient value lager than 60 Mm^{-1} as a "high value", lager than 40 Mm^{-1} and less than 60 Mm^{-1} as an "intermediate value" and less than 40 Mm^{-1} as a "low value". We can see that there are three different σ_a regions. It is clear that when wind comes from north with high speed (>4 m/s), σ_a is very low. When the wind blows from the same direction at low WS (0–2 m/s), the σ_a value is high, with a intermediate value when wind from south. In spring, the σ_a "high values" are in the WD sector from 330° to 60°. However, in summer, the high value region moves into the sector of 300° to 30°, and there are large areas with "intermediate value". In autumn, the high σ_a value appears in the sector extending from 210° to 60°, a much wider region. While in winter, the high σ_a region is focused on the region from 240° to 60° with low WS (0–2 m/s), and the highest value is much higher than the other seasons.

3.2 Scattering coefficient

As shown in Fig. 4, the diurnal variations of σ_s have the same pattern in summer and winter, which both have peaks around 10:00 a.m. and mid-night. However, the highest value in summer occurs at about 10:00, while, it occurs at mid-night in winter. The σ_s value in summer is larger than that in winter. What's more, the diurnal range is

ACPD
9, 11413–11440, 2009

lager in summer, and the peak in morning is much sharper. The σ_s peaks in morning may be attributed to large emission of aerosol and gaseous precursors (volatile organic compounds and NO_x) in the rush hour. Since mixing height varies with surface temperature, the diurnal variation of σ_s can be partly explained by changes in mixing height. The difference between summer and winter may be attributed to the secondary sulfates. Zheng et al. (2005) concluded that the secondary sulfates is the secondary lager contributor to $PM_{2.5}$ based on the observation conducted at five urban and rural sites in Beijing for one month in each quarter of year 2000. It is generally accepted that sulfate aerosols are the main contributor of radiation scattering in the atmosphere. Higher relative humidity in the summer allows more water to be picked up by hygroscopic component, resulting in increase of particle size, hence σ_s (Nessler et al., 2005).

Two-years mean σ_s value is 288±281 Mm^{-1} (Table 2). The σ_s in 2006 (310±281 Mm^{-1}) is larger than that in 2005 (264±279 Mm^{-1}). Although great effort was devoted to solve aerosol pollution in Beijing, σ_s still increases slightly. This can be ascribed to the fast economic growth, e.g. the amount of cars increase year after year. Weather system is another factor which can affect σ_s. From our wind analysis, the frequency of wind with speed (>8 m/s) in 2005 is larger than 2006. Besides, the frequency of precipitation in 2005 is also higher than that of 2006. Stronger wind and more precipitation may eliminate the pollutants. Seasonal variations are also shown in Table 2, with higher values in summer and autumn than those in spring and winter, and the highest occurs in summer. The production of secondary aerosol, which provides more hygroscopic component, and high relative humidity enhance the σ_s in summer (Sun et al., 2004). Compared with other observation, our result in summer (351±294 Mm^{-1}) is lower than the value of 488±370 Mm^{-1} obtained at Beijing in June, 1999 (Bergin et al., 2001) (Table 1). The result in spring (243±255 Mm^{-1}) is nearly two times of that in rural Beijing, but comparable with Silvia's (2002) observation in Mexico City.

Figure 5 presents the wind dependence of scattering coefficient. The definitions of

ACPD
9, 11413–11440, 2009

the figure are similar to Fig. 3 except that the color on the plot represents the magnitude of the scattering coefficient. Figure 5a, b, c and d are for spring, summer, autumn and winter respectively. It is clear that when wind blows from north or northwest with high speed (>4 m/s), σ_s is very low. And when the wind blows from the north with low speed (0–2 m/s), the σ_s is high. However, there exists some difference among four seasons. In spring, the large value of σ_s appears in the WD sector from 0° to 60° with the WS of 0–2 m/s. While in summer, the highest value region moves to the sector of 90° to 200° with the WS of 0–6 m/s, not only a wider but absolutely different direction region when compared with spring. Also, the highest σ_s value in summer is lager than that of spring. In autumn, the high σ_s value appears in the sector from 330° to 60° with the speed of 0–2 m/s. While in winter, the high σ_s region is only focused on the small region from 270° to 30°.

3.3 Single scattering albedo

As shown in Fig. 6, there are similar ω variation in summer and winter, which both peak around 14:00 and then decrease to a minimum before the sunrise. However, the lowest in summer appears earlier (05:00) than that in winter (07:00), and the ω increases faster in summer than that in winter. This diurnal pattern corresponds to the enhancement of scattering coefficient and the decrease of absorption coefficient in the morning. The diurnal range of ω in summer (0.75~0.85) is larger than that in winter (0.77~0.83). The mean ω values in winter are generally smaller than summer, except for early morning (00:00–07:00). It indicates the particles in summer are more absorptive than winter during 00:00–07:00, while less absorptive during 08:00–24:00. Meanwhile, the standard deviation in summer is also larger than that of winter.

As shown in Table 2, the yearly mean ω value is 0.82±0.07 in 2006, which is higher than that in 2005 (0.78±0.11), mainly because of the increasing of σ_s. The two-year mean ω value is 0.80±0.09. Our result is similar with the result of Bergin et al. (2001), lower than 0.9 at the wavelength of 440 nm from 33 months AERONET data (Xia et al., 2006) (Table 1). Qiu (2004) pointed out that the ω decreased from 0.851 to 0.803 at

Beijing during 1993–2001. Eck et al. (2005) reported ω at 550 nm in Beijing was 0.89 during 2001–2003 and saw a decrease since 2001.

Figure 7 displays the wind dependence of single scattering albedo. The definitions of the figure are similar to Fig. 3 except that the color on the plot represents the magnitude of the single scattering albedo. Figure 7a, b, c and d are for spring, summer, autumn and winter respectively. It can be seen in spring (Fig. 7a) when the wind blow from the southeast, the ω value is high. While when the wind is from northwest with low speed (0–4 m/s), the value of ω is low. However, in the same direction if the wind speed is high the ω will be lager. We can also see the high ω value appeared in the southeast wind with low wind speed in summer (Fig. 7b); while when the wind blows from north, the ω show a much lower value. The pattern in autumn (Fig. 7c) is similar with that of summer with the high ω value in the southeast wind and low value in the northwest wind. In winter (Fig. 7d), there are not obvious differences in different wind direction and wind speed.

Figure 8 shows the time series of two sectors selected from the polar coordinates. The red line represents the sector with WD between 120° and 180° and with WS of 0–4 m/s. The black line represents the sector of the WD between 300° and 360° and the same wind. Monthly averages are derived from hourly data which fall into the specific sectors. As can be seen in the figure, the red line is always above the black line and clearly illustrates the dependence of ω on wind direction; when the local wind direction is from 120°–180° (with 0–4 m/s wind) the particles are less absorptive than those when the local wind speed is from 300°–360° (with 0–4 m/s wind).

4 Discussions and conclusions

In this paper, we present results from a two-year aerosol ground-based observation in Beijing, a heavily polluted megacity. Based on the 24 months' data, three important parameters, including σ_a, σ_s and ω, are analyzed in terms of diurnal variation, seasonal variation and wind dependence. The overall mean values (and standard deviation)

ACPD
9, 11413–11440, 2009

for the entire time period (two years) for σ_a and σ_s as well as ω are 56±49 Mm^{-1}, 288±281 Mm^{-1} and 0.80±0.01, respectively. The ω in urban Beijing surface layer increased from 0.78±0.11 in 2005 to 0.82±0.07 in 2006, both are lower than the accepted observed ω range of 0.85–0.95 in Northern Hemisphere. To host the Olympic Games in 2008, the Beijing municipal government had made some policies to improve the air quality. σ_a is kept constant even though the development is fast which in part prove the policies work. However, σ_s still increases slightly, resulting in increase of ω. For the government, to control the secondary particulate pollution is still a big challenge.

σ_a, σ_s and ω illustrate characteristic diurnal variation. σ_a peaks in the night and its lowest value occurs in the noon and early afternoon. The diurnal pattern of σ_a could be ascribed to the evolution of boundary layer which is unstable in the daytime, along with the direct emission of BC in the night. Generally speaking, the stable boundary layer in night prohibits the dilution of pollutant, while the unstable boundary layer in daytime is beneficial for mixing of the pollutant. The main contributor of light absorption comes from black carbon which is mainly emitted from diesel truck. In Beijing, such trucks are restricted to night hours. As σ_s, it peaks around 10:00 and mid-night. The σ_s peaks in morning may be attributed to large emission of aerosol and gaseous precursors (volatile organic compounds and NO_x) in the rush hour. The evolution of boundary layer also affects the dilution of aerosols. Meanwhile, the σ_s in summer and autumn are higher than those in spring and winter, and the highest appears in summer. The production of secondary aerosol, which provides more hygroscopic component, and high relative humidity enhance the σ_s in summer. As ω, it peaks around 14:00 and then decrease to a minimum before the sunrise. The diurnal range of ω in summer (0.75~0.85) is larger than that in winter (0.77~0.83). The lowest in summer appears earlier (05:00) than that in winter (07:00). This diurnal pattern corresponds to the enhancement of scattering coefficient from late morning and the decrease of absorption coefficient from morning.

Meanwhile, σ_a, σ_s and ω show a wind dependence. Overall, the σ_a value is high-

ACPD
9, 11413–11440, 2009

est when the wind blows from north with low WS of 0–2 m/s. This indicates that an emission source may exist not far away from the sampling location to the north. From the magnitude we can see that Beijing is mainly governed by local source emission. However, both σ_a and σ_s are very low when wind blows from north with high speed. In winter, the highest σ_a value is higher than the other three seasons. Coal consumption for heating is a contributor to the high σ_a value in winter. σ_s experiences a similar dependence on local wind speed and direction as σ_a except during the summer. In summer, σ_s value is the highest when wind is from southeast with WS of 0–4 m/s. In the south of sample location, it is a highly polluted region. Along with the southeast wind, aerosol is brought to the sample location. σ_s has two regions where "high values" were observed: one is in the north with WS of 0–2 m/s, another is in the southeast with the WS of 0–4 m/s. As for ω, the value is higher in the sector of WD from 120°–180° with WS of 0–4 m/s than the sector of WD from 300°–360° with WS of 0–4 m/s. This may be due to a source or enhancement of absorbing aerosols in 300–360° direction. This wind dependence indicates that there is a good relationship between wind and aerosol optical properties. It would be helpful to take wind into consideration when enforce policies to improve air quality.

Acknowledgements. The study is partially supported by grants from the National Natural Science Foundation of China (NSFC) (No. 40575001 and No. 40775002) and the National High Technology Research and Development Program of China (863 Major Project, No: 2006AA06A303) of China.

References

Ando, M., Katagiri, K., Tamura, K., et al.: Indoor and outdoor air pollution in Tokyo and Beijing supercities, Atmos. Environ., 30, 695–702, 1994.

Arnott, W. P., Moosmuller, H., Sheridan, P. J., et al.: Photoacoustic and filter-based ambient aerosol light absorption measurements: Instrument comparisons and the role of relative humidity, J. Geophys. Res., 108(D1), 4034, doi:10.1029/2002JD002165, 2003.

Barnard, J. C., Kassianov, E. I., Ackerman, T. P., Johnson, K., Zuberi, B., Molina, L. T., and Molina, M. J.: Estimation of a "radiatively correct" black carbon specific absorption during the Mexico City Metropolitan Area (MCMA) 2003 field campaign, Atmos. Chem. Phys., 7, 1645–1655, 2007, http://www.atmos-chem-phys.net/7/1645/2007/.

Benjamin, G., Jean, C. R., Hélène, C., et al.: Impact of vertical atmospheric structure on Beijing aerosol distribution, Atmos. Environ., 40, 5167–5180, 2006.

Bergin, M. H., Cass, G. R., Xu, J., et al.: Aerosol radiative, physical, and chemical properties in Beijing during June 1999, J. Geophys. Res., 106(D16), 17969–17980, 2001.

Chan, C. K. and Yao, X. H.: Air Pollution in Mega Cities in China – a Review, Atmos. Environ., 42, 1–42, 2008.

Chu, D. A., Kaufman, Y. J., Zibordi, G., Chern, J. D., Mao, J., Li, C., and Holben, B. N.: Global monitoring of air pollution over land from the Earth Observing System-Terra Moderate Resolution Imaging Spectroradiometer (MODIS), J. Geophys. Res., 108(D21), 4661, doi:10.1029/2002JD003179, 2003.

Comrie, A.: A synoptic climatology of ozone pollution at three forest sites in Pennsylvania, Atmos. Environ., 28, 1601–1614, 1994.

Crutzen, P. J.: New directions: the growing urban heat and pollution "island" effects-impact on chemistry and climate, Atmos. Environ., 38, 3539–3540, 2004.

Eck, T. F., Holben, B. N., Dubovik, O., et al.: Columnar aerosol optical properties at AERONET sites in central eastern Asia and aerosol transport to the tropical mid-Pacific, J. Geophys. Res., 110, D06202, doi:10.1029/2004JD005274, 2005.

Eder, B., Davis, J. M., Bloomfield, P., et al.: An automated classification scheme designed to better elucidate the dependence of ozone on meteorology, J. Appl. Meterol., 33, 1182–1199, 1994.

Elminir, H. K.: Dependence of urban air pollutants on meteorology, Sci. Total Environ., 350, 225–237, 2005.

Hartog, J. J., Hoek, G., Mirme, A., et al.: Relationship between different size classes of particulate matter and meteorology in three European cities, J. Environ. Monitor., 7, 302–310, 2005.

He, K., Yang, F., Ma, Y., et al.: The characteristic of $PM_{2.5}$ in Beijing, China, Atmos. Environ., 35, 4954–4970, 2001.

IPPC, Intergovernmental Panel on Climate Change: Climate Change, in: The Scientific Basis,

edited by: Houghton, J. T., Ding, Y., Griggs, D. J., et al.: Cambridge Univ. Press, New York, USA, 2001.
Jacobson, M. Z.: Strong radiative heating due to the mixing state of black carbon in atmospheric aerosols, Nature, 409, 696–697, 2001.
Kaiser, D. P. and Qian Y.: Decreasing trends in sunshine duration over China for 1954–1998: Indication of increased haze pollution?, Geophys. Res. Lett., 29, 2042, doi:10.1029/2002GL016057, 2002.
Kaufman, Y. J., Tanré, D., Remer, L. A., Vermote, E. F., Chu, A., and Holben, B. N.: Operational remote sensing of tropospheric aerosol over land from EOS moderate resolution imaging spectroradiometer, J. Geophys. Res., 102(D14), 17051–17067, 1997.
Kaufman, Y. J., Tanré, D., and Boucher, O.: A satellite view of aerosols in the climate system, Nature, 419, 215–223, 2002.
Levy, R. C., Remer, L. A., Mattoo, S., Vermote, E. F., and Kaufman, Y. J.: Second-generation operational algorithm: Retrieval of aerosol properties over land from inversion of Moderate Resolution Imaging Spectroradiometer spectral reflectance, J. Geophys. Res., 112, D13211, doi:10.1029/2006JD007811, 2007.
Li, C. C., Mao, J. T., Lau, A. K., et al.: Research on the air pollution in Beijing and Surroundings with MODIS AOD products, Chinese Journal of Atmospheric Sciences, 27, 869–880, 2003 (in Chinese with English abstract).
Li, X. W., Zhou, X. J., Li, W. L.: The cooling of Sichuan Province in recent 40 years and its probable mechanisms, Acta Meteorologica Sinica, 9, 57–68, 1995.
Luo, Y. F., Lu, D., Zhou, X., et al.: Characteristics of the spatial distribution and yearly variation of aerosol optical depth over China in last 30 years, J. Geophys. Res., 106(D13), 14501–14513, 2001.
Mao, J. T. and Li, C. C.: Observation Study of Aerosol Radiative Properties over China, Acta Meteorologica Sinica, 20, 306–320, 2006.
Menon, S., Hansen, J., Nazarenko, L., and Luo, Y. F.: Climate effects of black carbon aerosols in China and India, Science, 297, 2250–2253, 2002.
Moosmuller, H., Arnott, W. P., Rogers, C. F., et al.: Photoacoustic and filter measurements related to aerosol light absorption during the Northern Front Range Air Quality Study (Colorado 1996/1997), J. Geophys. Res., 103(D21), 28149–28157, 1998.
Müller, D., Teche, M., Eichler, H., et al.: Strong particle light absorption over the Pearl River Delta (south China) and Beijing (north China) determined from combined Raman lidar and

Sun photometer observations, J. Geophys. Res., 33, L20811, doi:10.1029/2006GL027196, 2006.
Nessler, R., Weingartner, E., and Baltensperger, U.: Effect of humidity on aerosol light absorption and its implications for extinction and the single scattering albedo illustrated for a site in the lower troposphere, J. Aerosol Sci., 36, 958–972, 2005.
Penner, J. E., Dong X. Q., Chen Y.: Observational evidence of a change in radiative forcing due to the indirect aerosol effect. *Nature*, 427, 231-234, 2001.
Qian, Y. and Giorgi, F.: Regional climatic effects of anthropogenic aerosols? The case of southwestern China, Geophys. Res. Lett., 27, 3521–3524, 2000.
Qiu, J., Yang, L., and Zhang, X.: Characteristics of the imaginary part and single-scattering albedo of urban aerosols in northern China, Tellus, 56(B), 276–284, 2004.
Ramachandran, S. and Rajesh, T. A.: Black carbon aerosol mass concentration over Ahmedabad, an urban location in western India: Comparison with urban sites in Asia, Europe, Canada, and the United States, J. Geophys. Res., 112, D06211, doi:10.1029/2006JD007488, 2007.
Ramanathan, V., Crutzen, P. J., Kiehl, J. T., and Rosenfeld, D.: Aerosols, climate, and the hydrological cycle, Science, 294, 2119–2124, 2001a.
Ramanathan, V., Crutzen, P. J., Lelieveld, J., et al.: Indian Ocean Experiment: An integrated analysis of the climate forcing and effects of the great Indo-Asian haze, J. Geophys. Res., 106(D22), 28371–28398, 2001b.
Sun, Y. L., Zhuang, G. S., Wang, Y., et al.: The air-borne particulate pollution in Beijing - Concentration, composition, distribution and sources, Atmos. Environ., 38, 5991–6004, 2004.
Silvia, E. D.: Aerosol impacts on visible light extinction in the atmosphere of Mexico City, Sci. Total Environ., 287, 213–220, 2002.
Shi, Z., Shao, L., Jones, T. P., et al.: Characterization of airborne individual particles collected in an urban area, a satellite city and a clean air area in Beijing, Atmos. Environ., 37, 4097–4108, 2003.
Xia, X. A., Chen, H. B., Wang, P. C., et al.: Variation of column-integrated aerosol properties in a Chinese urban region, J. Geophys. Res., 111, D05204, doi:10.1029/2005JD006203, 2006.
Yan, P., Tang, J., Huang, J., Mao, J. T., Zhou, X. J., Liu, Q., Wang, Z. F., and Zhou, H. G.: The measurement of aerosol optical properties at a rural site in Northern China, Atmos. Chem. Phys., 8, 2229–2242, 2008,

http://www.atmos-chem-phys.net/8/2229/2008/.
Zhang, Y., Shao, L., Tang, K., et al.: The study of urban photochemical smog pollution, Acta Scientiarum Naturalium Universitatis Pekinensis, 34, 392–400, 1998 (in Chinese with English abstract).
Zheng, M., Salmon, L. G., Schauer, J. J., et al.: Seasonal trends in $PM_{2.5}$ source contributions in Beijing, China, Atmos. Environ., 39, 3967–3976, 2005.
Zhou, L. M., Dickinson, R. E., Tian, Y. H., et al.: Evidence for a significant urbanization effect on climate in China, P. Natl. Acad. Sci. USA, 101(26), 9540–9544, 2004.

Table 1. Aerosol optical properties made at different sites.

site	period	ω	σ_a(Mm^{-1})	σ_s(Mm^{-1})	instrumentation	reference
PKU, Beijing	1 week June, 1999	0.81±0.08 (550)	83±40 (565)	488±40 (530)	PSAP Nephlometer[a]	Bergin et al., 2001
IAP, Beijing	2001.03–05 2002.04–2004.10	~0.90 (440)	–	–	AERONET CIMEL radiometer	Xia et al., 2006
Beijing	1993–2001	0.851–0.803 (550)	–	–	Pyrheliometer pyranometer	Qiu et al., 2003
SDZ, Beijing(rural)	2003.09–2005.01	0.88 (525)	17.54±13.44 (525)	174.6±189.1 (525)	AE31[c] Nephelometer[b]	Yan et al., 2008
Beijing	2003.06	~0.89 (550)	–	–	AERONET CIMEL radiometer	Eck et al., 2005
PKU, Beijing	2005.01–2006.12	0.80±0.10 (525)	56 ±49 (532)	288 ±281 (525)	AE16[d] Nephelometer[b]	Our work
Hisar, India	2004.12	0.88 (500)	–	–	OPAC	Ramachandran et al., 2006
Gosan, South korea	2001.11	0.88±0.02 (550)	–	–		Kim et al., 2005
La Merced, Mexico City	1997.02.28–1997.03.10	0.72±0.08	80.8±31.9 (880)	225.3±132.8	AE-16[d] Nephelometer[e]	Silvia, 2002

The number in the parentheses represents the wavelength used in the measurement.
[a] Radiance Research nephelometer M903.
[b] Integrating Nephelometer (Model M9003, EcoTech, Australia).
[c] Aethalometer (Model AE31, Magee Scientific, USA).
[d] Aethalometer (Model AE16, Magee Scientific, USA).
[e] NGN-2 open-air integrating Nephelometer (Optec Inc).

ACPD
9, 11413–11440, 2009

Table 2. The averages of aerosol adsorption, scattering coefficient and single scattering albedo.

period	σ_a(Mm^{-1})	σ_s(Mm^{-1})	ω
Spring	45±39	243±255	0.81±0.10
Summer	54±40	351±294	0.82±0.11
Autumn	67±53	311±280	0.78±0.09
Winter	58±57	259±284	0.79±0.06
2005–2006	56±49	288±281	0.80±0.09
2005	58±52	264±279	0.78±0.11
2006	53±46	310±281	0.82±0.07

ACPD
9, 11413–11440, 2009

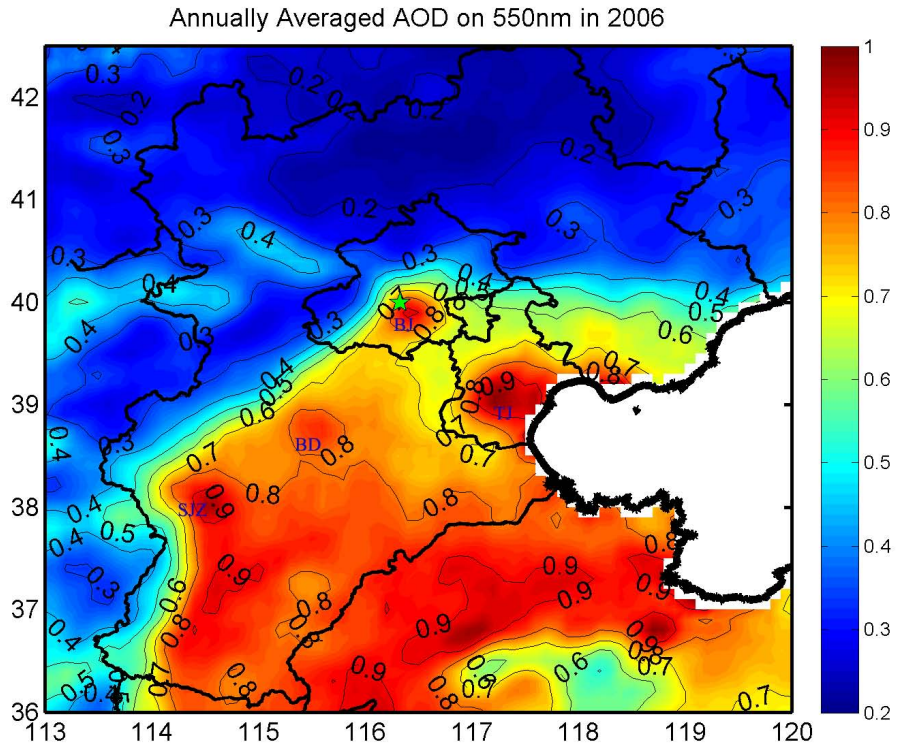

Fig. 1. Yearly mean AOD around Beijing in 2006.

ACPD

9, 11413–11440, 2009

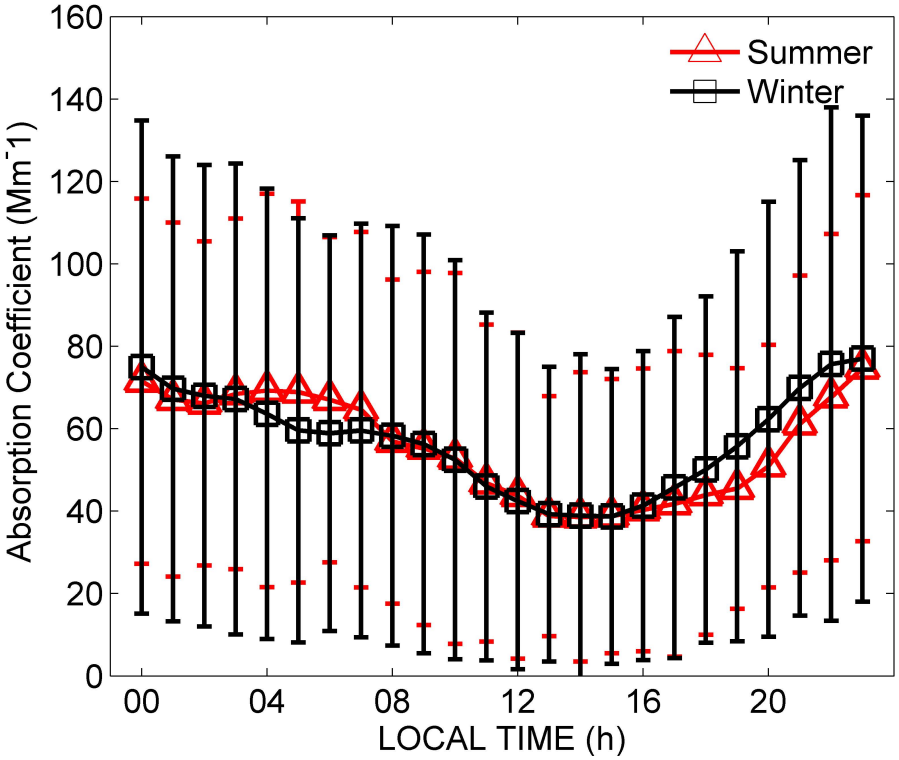

Fig. 2. Diurnal variation of absorption coefficient in summer and winter.

ACPD
9, 11413–11440, 2009

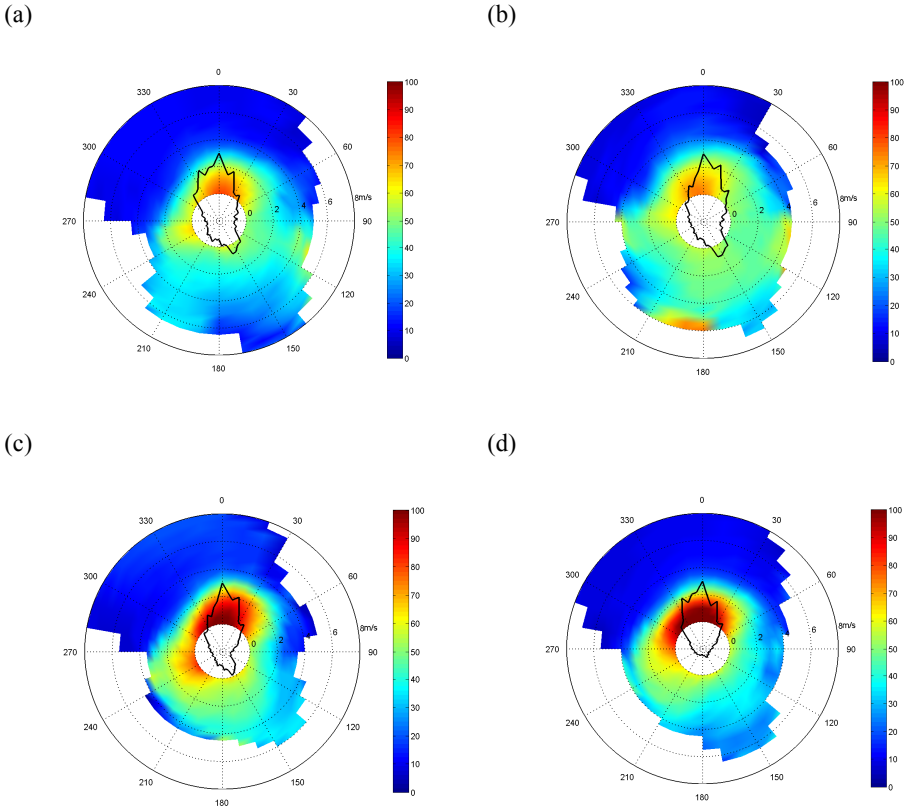

Fig. 3. Wind dependency of absorption coefficient.

ACPD
9, 11413–11440, 2009

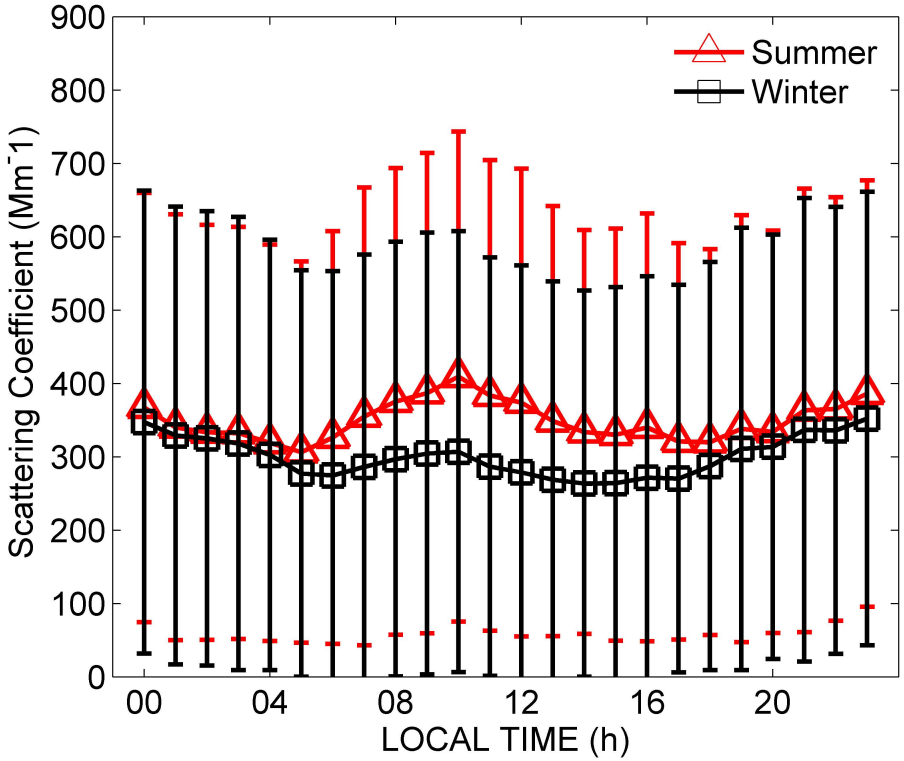

Fig. 4. Diurnal variation of scattering coefficient in winter and summer.

ACPD
9, 11413–11440, 2009

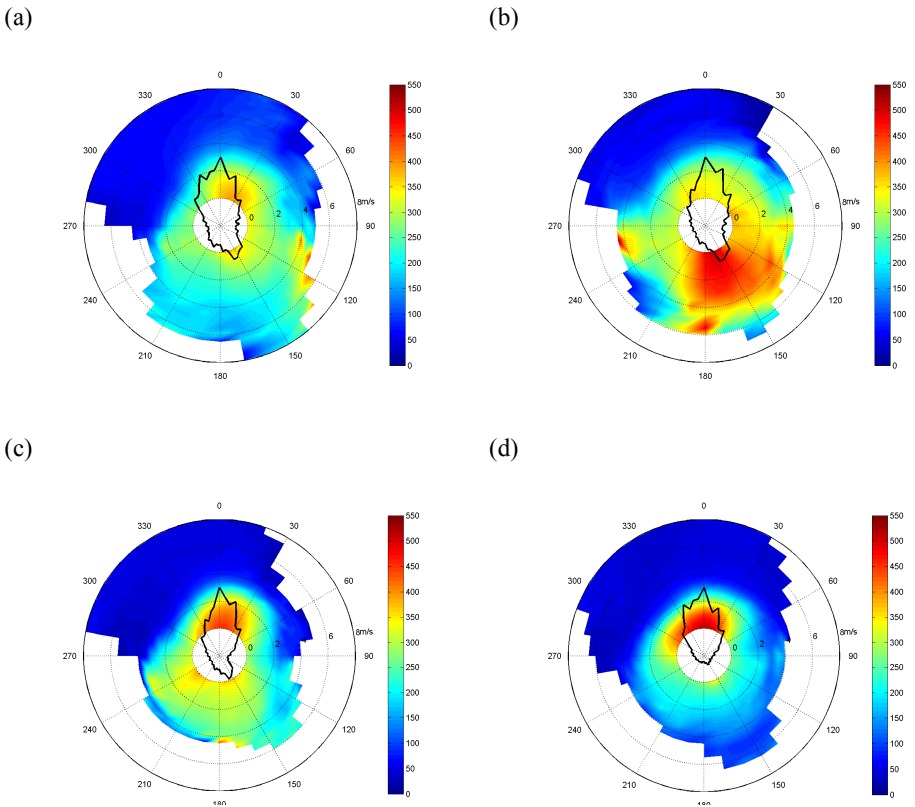

Fig. 5. Wind dependency of scattering coefficient.

ACPD
9, 11413–11440, 2009

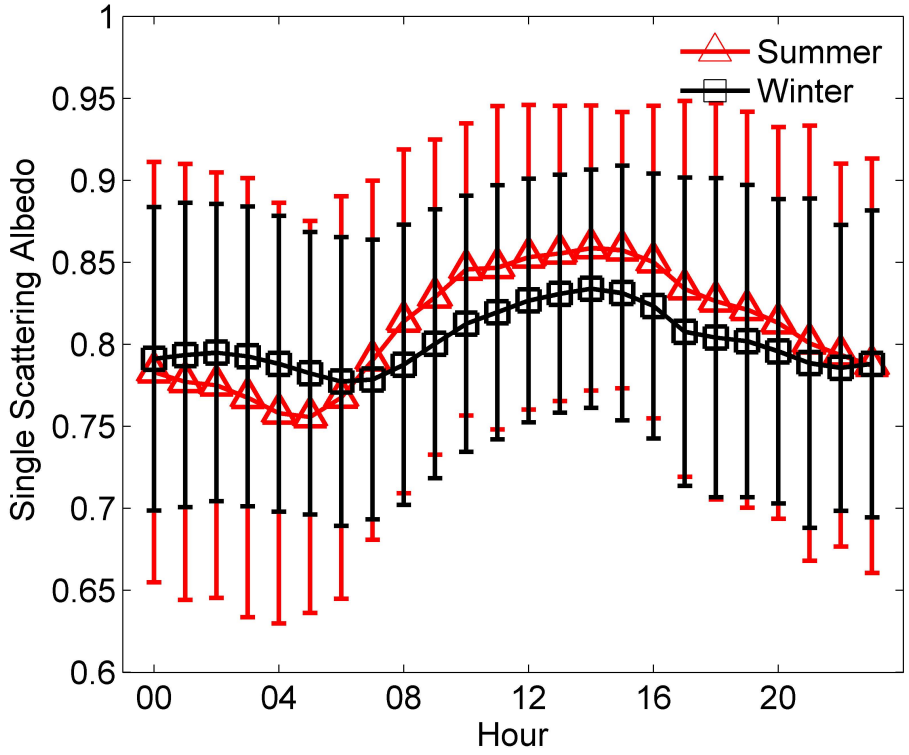

Fig. 6. Diurnal variation of SSA in summer and winter.

ACPD
9, 11413–11440, 2009

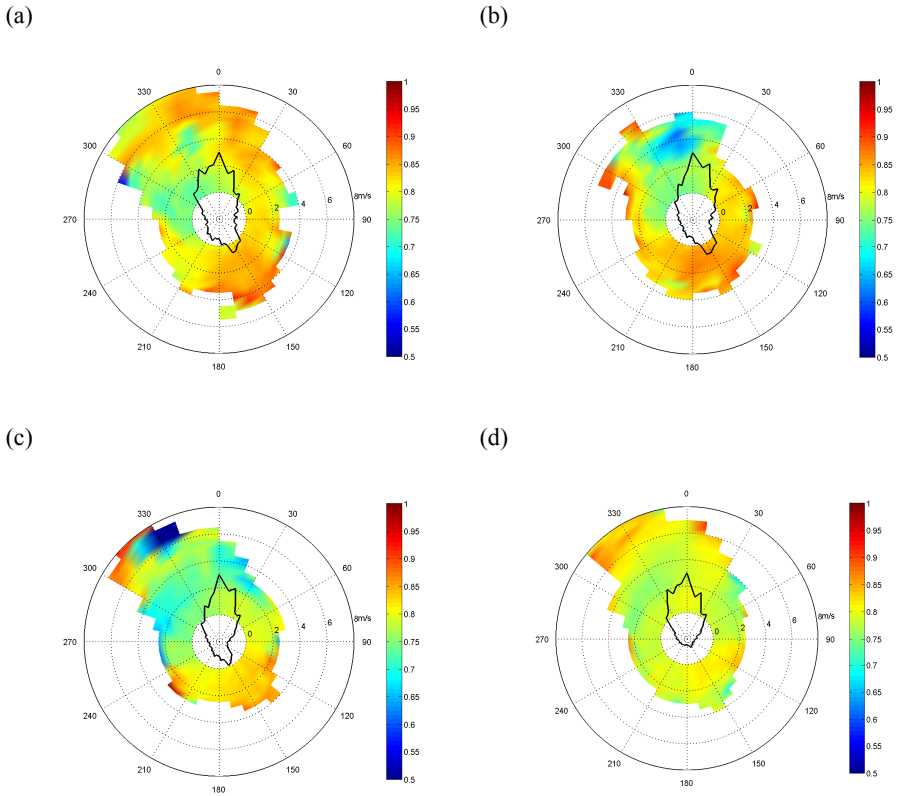

Fig. 7. Wind dependency of single scattering albedo.

ACPD
9, 11413–11440, 2009

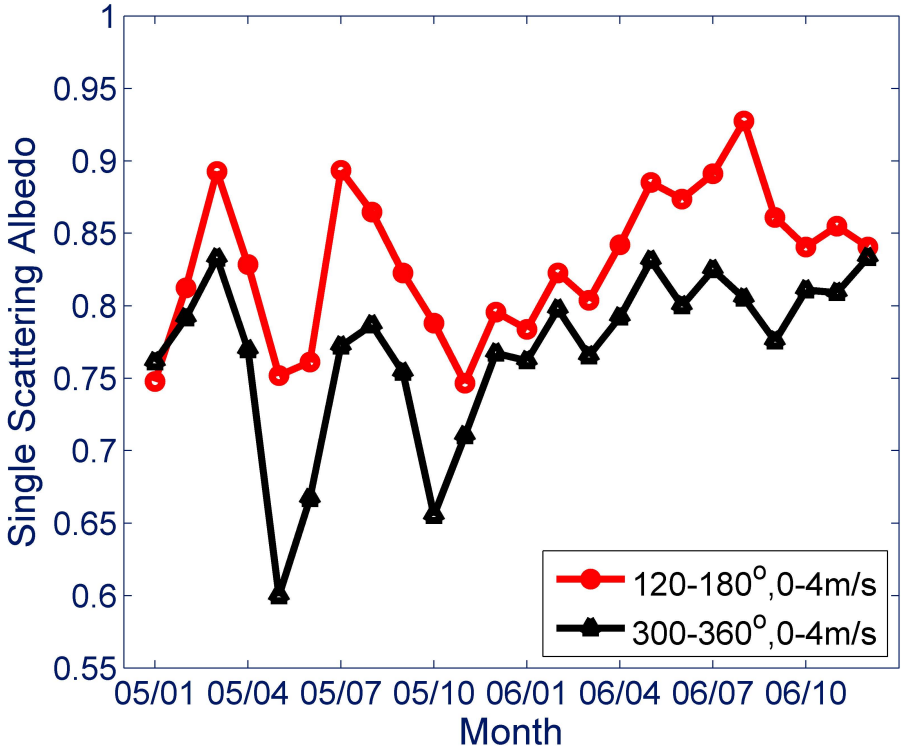

Fig. 8. Monthly mean SSA in two selected sectors.

ACPD
9, 11413–11440, 2009